Inorg. Chem. **2003**, *42*, 107−111

Inorganic Chemistry Article

Benzene Thermal Conversion to Nanocrystalline Indium Nitride from Sulfide at Low Temperature

Jianping Xiao, Yi Xie,* Rui Tang, and Wei Luo

Structure Research Laboratory and Department of Chemistry, University of Science and Technology of China, Hefei, Anhui 230026, P. R. China

Received June 30, 2002

A benzene thermal conversion route has been successfully developed to prepare nanocrystalline indium nitride at 180–200 °C by choosing $NaNH_2$ and In_2S_3 as novel nitrogen and indium sources. This route has been also extended to the synthesis of other group III nitrides. The product InN was characterized by X-ray diffraction (XRD), transmission electron microscopy (TEM) and high-resolution TEM, X-ray photoelectron spectroscopy (XPS), Raman spectroscopy, and infrared spectroscopy (IR). The optical properties of nanocrystalline InN were also recorded by means of UV–vis absorption spectroscopy and photoluminescence (PL) spectroscopy, indicating that the as-prepared sample was within the quantum confinement regime. Finally, the formation mechanism was also investigated.

Introduction

In the past decades, there has been much interest in the synthesis and characterization of the group III nitrides due to their fundamental physical properties as well as their potential applications as electronic and optoelectronic materials in device development.[1] The group III nitrides are ideal for high-power applications and utilization in caustic environments, because they are chemically inert, are resistant to radiation, and have large avalanche breakdown fields, high thermal conductivities, and large high-field electron drift velocities.[2] The group III nitrides and their alloys have been fabricated into various high-temperature and high-power microelectronic and optoelectronic devices.[2] However, the synthesis of the group III nitrides is especially difficult. Therefore, more and more efforts are made to develop novel synthetic routes of the group III nitrides.

Indium nitride, one of the group III nitrides, has currently acquired technological importance for blue/violet light-emitting diodes (LEDs) and laser diodes (LDs).[3] Furthermore, InN has promising transport and optical properties. Its large drift velocity at room temperature can render it better than GaAs and GaN for field effect transistors.[4] A tandem solar cell with an InN cell on the top and a Si cell at the bottom can theoretically achieve a maximum efficiency of 32.1%,[5] which is highly desirable for solar energy applications. However, among the group III nitrides, the growth of InN is the most difficult to achieve because of its low decomposition temperature (427−550 °C),[6] which makes the growth of InN most challenging. The growth of InN is particularly important because it has the lowest energy band gap (1.9 eV for InN, 3.4 eV for GaN, 6.2 eV for AlN[7]). By alloying InN into either AlN or GaN, the band gap of the semiconductor can be lowered into the 2−3 eV range, which is a critical range for making high-efficiency green and yellow visible light sources and detectors.

Conventional synthetic methods to semiconductor InN include organometallic precursor routes,[8] pyrolysis of In$(NH_2)_3$,[9] high-pressure direct synthesis,[10] atomic layer epi-

* E-mail: yxielab@ustc.edu.cn.

(1) (a) Morkoc, H.; Mohammad, S. N. *Science* **1995**, *267*, 51. (b) Morkoc, H.; Strite, S.; Gao, G. B.; Lin, M. E.; Sverdlov, B.; Burns, M. *J. Appl. Phys.* **1994**, *76*, 1363. (c) Matsuoka, T.; Ohki, T.; Ohno, T.; Kawaguchi, Y. *J. Cryst. Growth* **1994**, *138*, 727.
(2) Neumayer, D. A.; Ekerdt, J. G. *Chem. Mater.* **1996**, *8*, 25.
(3) (a) Matsuoka, T. *Adv. Mater.* **1996**, *8*, 469. (b) Ponce, F. A.; Bour, D. P. *Nature* **1997**, *386*, 351. (c) Nakamura, S. *Science* **1998**, *281*, 956.
(4) O'Leary, S. K.; Foutz, B. E.; Shur, M. S.; Bhapkar, U. V.; Eastman, L. F. *J. Appl. Phys.* **1998**, *83*, 826.
(5) Yamamoto, A.; Tsujino, M.; Ohkubo, M.; Hashimoto, A. *Sol. Energy Mater. Sol. Cells* **1994**, *35*, 53.
(6) (a) Jones, A. C.; Whitehouse, C. R.; Roberts, J. S. *Chem. Vap. Deposition* **1995**, *1*, 65. (b) Akasaki, I.; Amano, H. *J. Cryst. Growth* **1995**, *146*, 455.
(7) Strite, S.; Morkoc, H. *J. Vac. Sci. Technol. B* **1992**, *10*, 1237.
(8) (a) Dingman, S. D.; Rath, N. P.; Markowitz, P. D.; Gibbons, P. C.; Buhro, W. E. *Angew. Chem., Int. Ed. Engl.* **2000**, *39*, 1470. (b) Fischer, R. A.; Sussek, H.; Miehr, A.; Pritzkow, H.; Herdtweck, E. *J. Organomet. Chem.* **1997**, *548*, 73. (c) Bae, B.; Park, J. E.; Kim, B.; Park, J. T. *J. Organomet. Chem.* **2000**, *616*, 128. (d) Fischer, R. A.; Miehr, A.; Metzger, T.; Born, E.; Ambacher, O.; Angerer, H.; Dimitrov, R. *Chem. Mater.* **1996**, *8*, 1356.
(9) Purdy, A. P. *Inorg. Chem.* **1994**, *33*, 282.
(10) Bo'ckowski, M. *Physica B* **1999**, *265*, 1.

10.1021/ic0258330 CCC: $25.00 © 2003 American Chemical Society

Published on Web 12/06/2002

taxy,[11] reactive magnetron sputtering,[12] chemical vapor deposition (CVD),[13] melt synthesis,[14] halogen-transport vapor phase epitaxy (VPE),[15] and molecular beam epitaxy (MBE).[16] All these reported routes are very useful and are of widespread importance, but there are some limitations to their realization. For example, some methods require either high processing temperature, high posttreatment temperature, high pressure, complex organometallic reactions and toxic gases, or some extreme reaction conditions such as an absolute nonaqueous and non-oxygen environment. Over the past years, there have been considerable efforts to explore new reaction routes to the group III nitrides under milder synthetic conditions. Previously, crystalline GaN was successfully prepared via a benzene thermal route using the reaction of Li_3N and $GaCl_3$ in our research group.[17] However, InN could not be obtained via a similar route using the reaction of Li_3N and InX_3 (X = Cl, Br), which yielded InX and elemental indium.[18]

Herein, we report a novel conversion route to the synthesis of nanocrystalline InN from sulfide at low temperature. The reaction is carried out in a benzene solution at 180−200 °C. The temperature used is, to the best of our knowledge, the lowest temperature at which crystalline InN has been obtained, far below its decomposition range. In addition, complex organometallic reactions, toxic gases, or extreme reaction conditions to crystalline semiconductor InN have been completely avoided. The reaction used in our approach can be formulated as follows:

$$In_2S_3 + 6NaNH_2 \rightarrow 2InN + 3Na_2S + 4NH_3$$

Experimental Section

Synthesis of Nanocrystalline InN. In a typical procedure, a stoichiometric mixture of In_2S_3 prepared according to the previously reported method[19] and analytically pure $NaNH_2$ was added into a 50-mL Teflon-lined autoclave, which was then filled with benzene up to 95% of the total volume. The autoclave was sealed and maintained at 180−200 °C for 15 h, then allowed to cool to room temperature naturally. The black precipitate was filtered off, washed with dilute acid, absolute ethanol, and distilled water in sequence, and then dried under vacuum at 50 °C for 4 h.

Structure, Composition, and Optical Properties Characterization. X-ray diffraction (XRD) analysis was carried out with a Japan Rigaku D/max-rA X-ray diffractometer with graphite monochromatized Cu Kα radiation (λ = 1.541 78 Å). The scan rate of 0.05 deg/s was used to record the patterns in the 2θ range of 20−80°. The transmission electron microscopy (TEM) image and selected area electron diffraction (SAED) pattern were taken on a Hitachi Model H-800 transmission electron microscope with an accelerating voltage of 200 kV. The structure and lattice image of nanocrystalline InN was studied by using a JEOL-2010 high-resolution transmission electron microscope (HRTEM). Energy-dispersive X-ray spectrum (EDS) analysis was employed for composition determination. Samples for the electron microscope were prepared by 1 h ultrasonic dispersion of 0.1 g of the as-prepared powder with 10 mL of ethanol in a 30-mL conical flask. Then, the suspension was dropped onto a conventional carbon-coated copper grid and dried in air before performance.

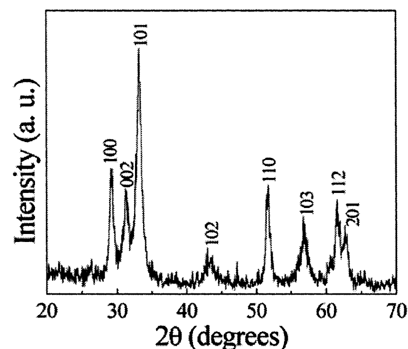

Figure 1. XRD pattern of the as-obtained product.

X-ray photoelectron spectroscopy (XPS) was performed on an ESCALab MKII X-ray photoelectron spectrometer, using Mg Kα X-ray as the excitation source. The binding energies obtained in the XPS analysis were calibrated against the C 1s peak at 284.6 eV. Room-temperature Raman spectra were taken with a Spex 1403 Raman spectrometer, equipped with an Ar^+ ion laser as a light source operating at a wavelength of 514.5 nm and focused on the sample through an optical microscope. The infrared spectrum was recorded in the wavenumber range of 4000−400 cm^{-1} with a Nicolet Model 759 Fourier transform infrared (FTIR) spectrometer, using a KBr wafer. UV−vis absorption spectroscopy was taken on a JGNA Specord 200 PC UV−vis spectrophotometer when ethanol was used as a reference. Photoluminescene experiments were carried out on a Hitachi 850 fluorescence spectrometer with a Xe lamp at room temperature.

Results and Discussion

XRD was used to examine the crystal structure of the sample. Figure 1 shows a typical XRD pattern of the product prepared via the benzene thermal conversion process. All the diffraction peaks can be indexed to be a pure hexagonal phase InN with high crystallinity. The refined lattice parameters $a = 3.551 \pm 0.004$ Å and $c = 5.716 \pm 0.006$ Å are extracted from the XRD data, which agree with the literature values of a = 3.54 Å and c = 5.705 Å.[20] No impurity peaks from elemental In, In_2O_3, or In_2S_3 were found in the experimental range. From the width of the XRD peaks, the average crystalline dimension of the product is estimated to be 10 nm according to the Scherrer equation.[21] IR spectroscopy (Figure 2) was carried out to examine the purity of the product and indicated the absence of both NH and

(11) Inushima, T.; Shiraishi, T.; Davydov, V. Y. *Solid State Commun.* **1999**, *110*, 491.
(12) (a) Takai, O.; Ikuta, K.; Inoue, Y. *Thin Solid Films* **1998**, *318*, 148. (b) Ikuta, K.; Takai, O.; Inoue, Y. *Thin Solid Films* **1998**, *334*, 49.
(13) Parala, H.; Devi, A.; Hipler, F.; Maile, E.; Birkner, A.; Becker, H. W.; Fischer, R. A. *J. Cryst. Growth* **2001**, *231*, 68.
(14) Grzegory, I.; Jun, J.; Bockowski, M.; Krukowski, St.; Wróblewski, M.; Lucznik, B.; Porowski, S. *J. Phys. Chem. Solids* **1995**, *56*, 639.
(15) (a) Takahashi, N.; Ogasawara, J.; Koukitu, A. *J. Cryst. Growth* **1997**, *172*, 298. (b) Igaracshi, O. *Jpn. J. Appl. Phys.* **1992**, *31*, 2665.
(16) (a) Lu, H.; Schaff, W. J.; Hwang, J.; Wu, H.; Koley, G.; Eastman, L. F. *Appl. Phys. Lett.* **2001**, *79*, 1489. (b) Aderhold, J.; Davydov, V. Y.; Fedler, F.; Klausing, H.; Mistele, D.; Rotter, T.; Semchinova, O.; Stemmer, J.; Graul, J. *J. Cryst. Growth* **2001**, *222*, 701.
(17) Xie, Y.; Qian, Y. T.; Wang, W. Z.; Zhang, S. Y.; Zhang, Y. H. *Science* **1996**, *272*, 1926.
(18) Wells, R. L.; Janik, J. F. *European J. Solid State Inorg. Chem.* **1996**, *33*, 1079.
(19) Yu, S. H.; Shu, L.; Qian, Y. T.; Xie, Y.; Yang, J.; Yang, L. *Mater. Res. Bull.* **1998**, *33*, 717.
(20) JCPDS Cards No. 2-1450 for InN.
(21) Wagner, C. N. J.; Aqua, E. N. *Adv. X-Ray Anal.* **1964**, *7*, 46.

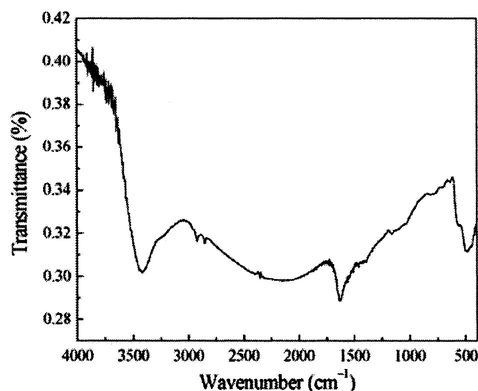

Figure 2. Typical IR spectrum of the as-obtained product.

NH_2 groups, suggesting a high degree of purity. The IR spectrum of the product showed a broad absorption at ca. 510 cm^{-1}, assignable to the In−N stretch.[22] Further evidence for the purity and composition of the sample was obtained by XPS measurements. The survey spectrum indicates the presence of In and N as well as C from the reference and O impurity from absorbed gaseous molecules and the absence of any impurity such as S or Na. Higher resolution spectra were also recorded in the In 3d and N 1s regions. Figure 3 shows the XPS spectra of the sample. The In core spin−orbit split to the $3d_{5/2}$ peak at 444.3 eV and $3d_{3/2}$ peak at 451.9 eV. The peak at around 397.5 eV corresponds to N 1s of InN. These results are close to the reported values for bulk InN.[23] No obvious peaks for indium oxide, indium sulfide, elemental In, or other impurities were observed. Therefore, XPS further confirms the formation of InN. The quantification of the XPS peaks gives a In:N ratio of 1.05: 1, which is close to the stoichiometry of InN.

To investigate the morphology and size of the product, it was mounted on the grid of a transmission electron microscope. A typical TEM image of the sample is shown in Figure 4a. The as-obtained nanocrystalline InN has rodlike and platelike morphologies. The size of the particles ranges from 10 to 30 nm, which is generally consistent with the XRD analysis. Furthermore, the highly crystalline nature of the product was confirmed by the SAED pattern shown in Figure 4b. The diffraction rings/spots can be again indexed as (100), (002), (101), (110), (103), and (112) reflections, according to the hexagonal structure of polycrystalline InN, which further supports the XRD result. HRTEM was applied to study further the detailed structure of nanocrystalline InN. As shown in Figure 5, the lattice spacing of the area *A* is measured to be 3.07 Å, which corresponds to the (100) plane in hexagonal InN. The prominent lattice spacing calculated from the area *B* is 2.70 Å, which is assigned to the (101) plane in hexagonal InN. The nanocrystalline feature observed in the HRTEM image is distinctive to hexagonal indium nitride. The EDS recorded on the InN nanocrystallites is illustrated in Figure 6, indicating that the presence of In and N as well as a Cu peak from the TEM grid and an O peak from absorbed gaseous molecules. No peaks from S and other impurities are observed, which reveals that there is no residual impurity in the product. The quantitative calculation of EDS peaks indicates that the atomic ratio of In to N is 1.03:1, which is close to the result of the XPS measurement.

Raman spectroscopy was used to characterize the as-obtained product. The zinc blende structure has only two Raman-active phonons F_2(TO) and F_2(LO), while the wurtzite structure has six Raman-active phonons: A_1(TO), A_1(LO), E_1(TO), E_1(LO), and $2E_2$.[24] Therefore, the number of peaks observed in the Raman spectra indicates whether the wurtzite phase is present or not. Figure 7 shows a typical Raman spectrum of the sample. The hexagonal InN related peaks at 443, 488, and 588 cm^{-1} are attributed to the A_1(TO) mode, E_2 mode, and A_1(LO) mode, respectively. The Raman spectrum agrees well with other reports in the literature for InN thin films[25] as well as polycrystalline InN.[26] In a word, the result derived from the Raman spectrum further confirms the presence of the hexagonal phase of InN in the product, which is consistent with the XRD conclusion.

All the above characterization results have confirmed that nanocrystalline InN with a hexagonal phase has been successfully prepared via our designed reaction route. Then what factors play important roles in the formation of nanocrystalline InN? It is well-known that choosing reactive sources is vital to the establishment of novel synthetic routes. It was reported that the ionic nitrides could be prepared by loss of ammonia from amide on heating,[27] which enlightens us on attempting to make $NaNH_2$ transform to Na_2NH and Na_3N by loss of ammonia on heating. The renascent Na_3N can be regarded as a good kind of nitrogen source due to its high reactivity. Then what is chosen as the indium source? It is well-known that InX_3 very easily hydrolyses even on weighing in the air and is reduced to elemental indium once it encounters strong reducing agents such as $NaNH_2$ or Li_3N. In the contrast, anhydrous In_2S_3 is very easily available. In addition, as far as In_2S_3 with strong covalent ability is concerned, it is not easy to be reduced to elemental indium, although $NaNH_2$ is a strong reducing agent, which can guarantee the metathesis of In_2S_3 and the renascent Na_3N in the benzene thermal system. Therefore, In_2S_3 instead of InX_3 is chosen as the novel indium source in our strategy, and the reaction used in our approach can be formulated as follows:

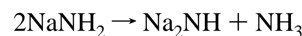

$$2NaNH_2 \rightarrow Na_2NH + NH_3$$

$$NaNH_2 + Na_2NH \rightarrow Na_3N + NH_3$$

(22) Nakamoto, K. *Infrared and Raman of Inorganic and Coordination Compounds*, 3rd ed.; Wiley: New York, 1978.

(23) Lu, Y.; Ma, L.; Lin, M. C. *J. Vac. Sci. Technol. A* **1993**, *11*, 2931.

(24) Agulló-Rueda, F.; Mendez, E. E.; Bojarczuk, B.; Guha, S. *Solid State Commun.* **2000**, *115*, 19.

(25) (a) Lee, M. C.; Lin, H. C.; Pan, Y. C.; Shu, C. K.; Ou, J.; Chen, W. H.; Chen, W. K. *Appl. Phys. Lett.* **1998**, *73*, 2606. (b) Davydov, V. Y.; Emtsev, V. V.; Goncharuk, I. N.; Smirnov, A. N.; Petrikov, V. D.; Mamutin, A. F.; Vekshin, V. A.; Ivanov, S. V. *Appl. Phys. Lett.* **1999**, *75*, 3297.

(26) Dyck, J. S.; Kim, K.; Limpijumnong, S.; Lambrecht, W. R. L.; Kash, K.; Angus, J. C. *Solid State Commun.* **2000**, *114*, 355.

(27) Cotton, F. A.; Wilkinson, G.; Murillo, C. A.; Bochmann, M. *Advanced Inorganic Chemistry*, 6th ed.; John Wiley & Sons: 1999; p 316.

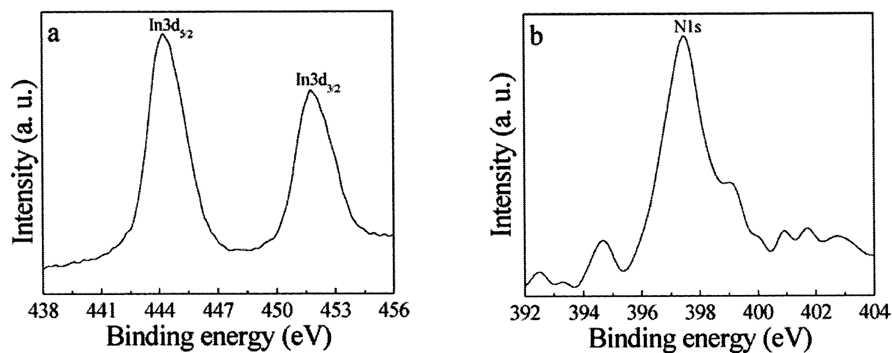

Figure 3. Higher resolution XPS spectra of the sample: (a) **3d** region; (b) N 1s region.

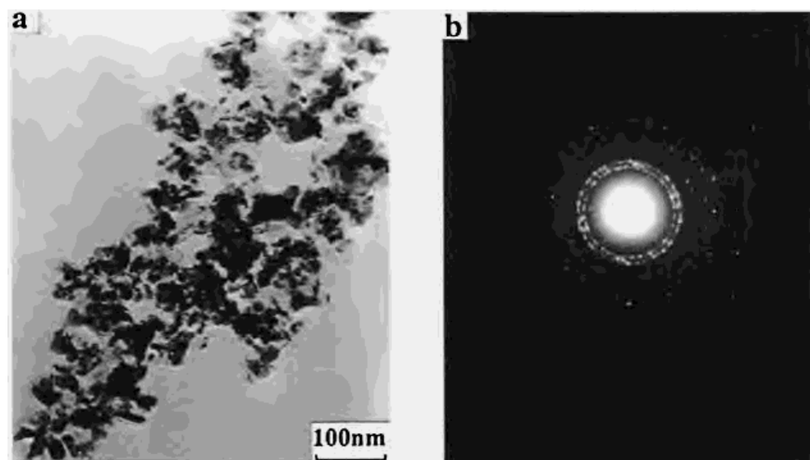

Figure 4. (a) TEM image of the as-obtained product. (b) The Corresponding SAED pattern.

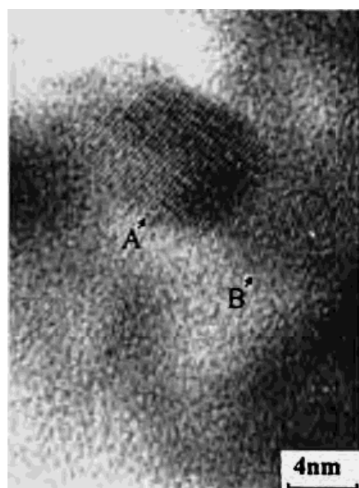

Figure 5. HRTEM image of InN nanocrystallites.

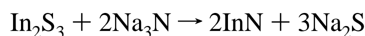

$$In_2S_3 + 2Na_3N \rightarrow 2InN + 3Na_2S$$

However, the formation of crystalline indium nitride may be complex and needs further investigation. Since the target InN is derived from indium sulfide in the benzene thermal solution, we call this synthetic method the benzene thermal conversion route. This method can be extended to the synthesis of other group III nitrides. By substituting In_2S_3 with Al_2S_3 or Ga_2S_3, we have also obtained AlN and GaN semiconductors. The results of the synthesis of nitrides through the benzene thermal conversion process are summarized in Table 1.

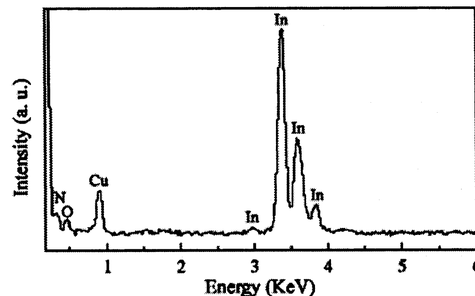

Figure 6. EDS analysis of InN nanocrystallites. Cu is from the HRTEM grid and O is from absorbed gaseous molecules.

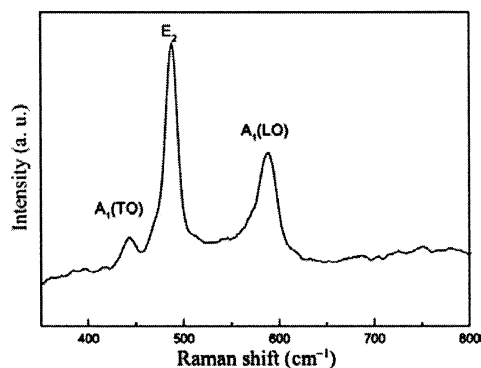

Figure 7. Typical Raman spectrum of the sample.

Finally, the optical properties of the as-obtained InN nanocrystallites were investigated by UV−vis absorption spectroscopy and photoluminescence (PL) spectroscopy at room temperature. From the absorption spectrum shown in

Table 1. Summary of the Results of the Synthesis of Nitrides by the Benzene Thermal Conversion Route from Sulfides

reactant	condition	product	color	particle size
$NaNH_2 + In_2S_3$	180 °C/15 h	crystallized InN	black	10−30 nm
	200 °C/15 h	crystallized InN	black	10−40 nm
$NaNH_2 + Al_2S_3$	180 °C/15 h	poorly crystallized AlN	brown	8−15 nm
	230 °C/15 h	crystallized AlN	black	10−25 nm
$NaNH_2 + Ga_2S_3$	180 °C/15 h	amorphous GaN	black	10−15 nm
	230 °C/15 h	poorly crystallized GaN	black	15−25 nm

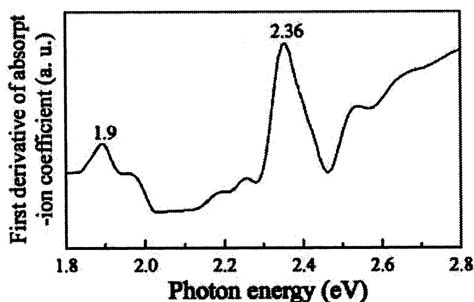

Figure 8. Absorption spectrum of the as-prepared InN nanocrystallites.

Figure 8, we can see that two peaks are present in the spectrum. The peak at 1.9 eV can be assigned to the band gap transition, being an absorption onset of bulk InN. The band at around 2.36 eV is a feature not seen in the spectrum of the bulk material, which can be attributed to the blue shift due to the small size of InN nanocrystallites. While the absorption spectrum confirms the existence of the InN particles within the quantum-confined regime, the PL spectrum can provide additional information. The spectrum shown in Figure 9 clearly indicates a broad peak at 2.2 eV, with the blue shift of 0.3 eV compared to the band gap emission. Therefore, these features indicate the quantum-confined effects of the as-obtained InN nanocrystallites.

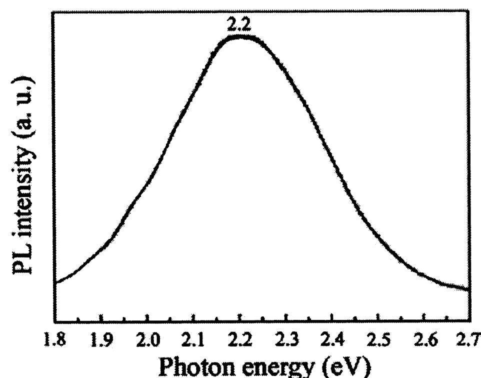

Figure 9. Room-temperature PL spectrum of the sample.

Conclusions

In summary, we describe a novel benzene thermal conversion route to the group III nitrides from sulfides. By choosing $NaNH_2$ and In_2S_3 as novel nitrogen and indium sources, we have achieved the growth of nanocrystalline InN under very mild reaction conditions. The formation mechanism was also studied to indicate that it proceeds with Na_3N as the probable intermediate. We believe that this simple method has potential applications in synthesizing other group nitrides.

Acknowledgment. Financial support from the Chinese National Science Foundation of Natural Science Research and the Chinese Ministry of Education are gratefully acknowledged.

IC0258330